A Modified Method to Calculate Dual Isotope Slopes for the Natural Attenuation of Organic Pollutants in the Environment

Jin-Ru Feng
Peking University
Hong-Gang Ni (nihg@pkusz.edu.cn)
Peking University https://orcid.org/0000-0003-2331-2667

Research Article

Keywords: Biodegradation, Two-dimensional isotope fractionation, Mechanism insight, One-sample t test, Compound specific isotope analysis

Posted Date: February 15th, 2021

DOI: https://doi.org/10.21203/rs.3.rs-180409/v1

A modified method to calculate dual isotope slopes for the natural attenuation of organic pollutants in the environment

Jin-Ru Feng and Hong-Gang Ni*

School of Urban Planning and Design, Shenzhen Graduate School, Peking University, Shenzhen 518055, P. R. China

Corresponding author. Tel.: +86-755-26033017; Fax: +86-755-26032801. E-mail address: nihg@pkusz.edu.cn

Abstract

Two-dimensional compound specific isotope analysis has become a powerful tool to distinguish reaction mechanism. Lambda (Λ), an essential and important parameter for processing two-dimensional isotope fractionation data, is specific to a reaction mechanism. In the present article, we modified the existing algorithms for Lambdas based on the review of the current methods. Specifically, through regressing $[(1000+\delta E_{0,2})*(n_1*x_2)*\Delta\delta E_{bulk,1}]$ versus $[(1000+\delta E_{0,1})*(n_2*x_1)*\Delta\delta E_{bulk,2}]$ by York method, a novel method was developed to calculate Λs. The improved method eliminates both the influence of non-reacting position and the initial isotope signatures. Furthermore, this method retains the advantages of two-dimension isotope plot, which eliminates contributions from commitment to catalysis, no need to determine fraction of remaining substrate and can be constructed even from filed data. At the same time, one sample *t* test is applied to generate 95% confidence interval of data set of Λ_{ri}s for various reaction mechanisms. The range of 5.67–24.8, 8.54–9.80, 0.51–8.35, 25.2–36.8, 7.09–21.9 are responsible for oxidation of C-H bonds (Z_C=1, Z_H=3), oxidation of C-H bonds (Z_C=1,Z_H=4), aerobic biodegradation of benzene (Z_C=6,Z_H=6), methanogenic or sulfate-reducing biodegradation of benzene (Z_C=6,Z_H=6), and nitrate-reducing biodegradation of benzene (Z_C=6,Z_H=6). The accumulation and correction of these values will make the data measured in the field easier to interpret.

Keywords Biodegradation; Two-dimensional isotope fractionation; Mechanism insight; One-sample *t* test; Compound specific isotope analysis

32

Introduction

Compound specific isotope analysis (CSIA) has been extensively explored as a useful tool to identify contaminant sources and monitor the extent of pollutant degradation (Elsner 2010, Elsner &Imfeld 2016). By measuring kinetic isotopic effects (KIEs) of biochemical reactions for compounds, CSIA also can be provided insight into biodegradation reaction mechanisms (Elsner et al. 2007). KIEs for a specific reaction mechanism are fully expressed only if the dominant isotope fractionation step is the slowest step, known as the rate-determining step or rate-limiting step (Jaekel et al. 2014). However, the isotope-sensitive step (*i.e.*, the bond conversion) is occasionally preceded by a not or slightly fractionation process such as transport and adsorption to reactive sites, or formation of enzyme-substrate complexes, which will make the measured apparent kinetic isotope effect smaller than the intrinsic KIE (Elsner et al. 2005, Feisthauer et al. 2011). The masking factors mainly include high microbial cell densities, low substrate or electron acceptor bioavailability, substrate transport across cellular membranes and the reversibility of enzymatic reactions, respectively (Jaekel et al. 2014). The expression "commitment to catalysis" (Northrop 1981) was introduced to describe this influence. To mitigate masking effects of biochemical reactions, measure of isotope signatures of two elements involved the isotope-sensitive steps simultaneously (two dimensional CSIA) has been proposed (Fischer et al. 2007, Jaekel et al. 2014). The slope of a dual-isotope plot, Lambda (Λ), can be specific to one certain reaction mechanism.

Generally, four methods are used to calculate Λs as follows:

(i) Calculating Λs from fractionation factor at the reacting position (α_{rp}) (Elsner et al. 2005). When there are heavy isotopes in the reaction site of the molecule, α_{rp} usually be masked by commitment to catalysis (C) and the influence of C can be described by Eq. (1) (Elsner et al. 2005),

$$(\alpha_{rp}^{\subset})^{-1} = \frac{C+(\alpha_{rp}^{\not\subset})^{-1}}{C+1} \quad (1)$$

where the superscript "$\subset$" and "$\not\subset$" represent the presence of commitment to catalysis and not. As masking effects always equally the two elements involved in the biochemical reactions (Elsner et al. 2005, Zwank et al. 2005), the combination of two-dimensional isotope equations elegantly eliminates contributions from commitment to catalysis shown in Eq. (2).

$$\Lambda_{\alpha} = \frac{(\alpha_{rp,H})^{-1}-1}{(\alpha_{rp,C})^{-1}-1} \quad (2)$$

(ii) Calculating Λs and its uncertainty by dual-isotope plots that use regression with ordinary linear regression (OLR). The rate limiting step of non-fractionation including the substrate absorbed by cells or combined with enzyme caused by enzyme masking effect has the equal effect on the isotopic effect of different elements. Therefore, the masking effect of commitment to catalysis can be reduced to a certain extent with the ratio

calculation. Isotope signatures of different elements (δE_1, δE_2) could be plotted on the horizontal and vertical coordinates respectively and the slope of $\Delta\delta E_1$ versus $\Delta\delta E_2$, denoted by Λ_{OLR}, is obtained from OLR. To eliminate the influence of the initial isotope signatures δE_0, the change in isotope signature at time t ($\Delta\delta E_t = \delta E_t - \delta E_0$) is utilized in the two-dimensional isotope plot, rather than measured isotope signature δE_t.

(iii) Calculating Λs and its uncertainty by dual-isotope plots that use regression with York method (Ojeda et al. 2019). Plotting dual-isotope, OLR only minimizes the sum of squares of one type of isotope signature set as *y*-variable, without considering the measurement error of another one. While measurement errors are inherent to both variables and neither of them could be ignored. Λ_{york} is obtained by regressing measured data through the York method that incorporates uncertainty in both isotope measurements (Ojeda et al. 2019), then Λ_{york} as a more appropriate estimation of Lambda than Λ_{OLR} was proposed.

(iv) In addition to the above, there is another way to calculate Λ (Eq. (3)) (Jaekel et al. 2014).

$$\Lambda_{rp} = \frac{\varepsilon_{rp,1}}{\varepsilon_{rp,2}} \quad (3)$$

95 Where $\varepsilon_{rp,1}$ and $\varepsilon_{rp,2}$ are isotopic enrichment factors in the reactive positions for the
96 two isotopes.
97
98 To our best knowledge, there is limited comprehensive and in-depth comparison among
99 these four methods for data processing yet. Still, there remains the puzzling disparity
100 among the Λs calculated with the current four methods. The objective of this paper is to
101 propose a modified method for Λs calculation which can make the field survey data
102 easily to interpret.
103
104 **Methods**
105 **Data collection**
106 Published studies using dual isotope (C, H) fractionation for practitioners to identify
107 transformation mechanisms are far more than other isotopes. This provided a good
108 opportunity to evaluate the uncertainty associated with the current mathematical models
109 with carbon and hydrogen isotopes. Experimental data were collected from previous
110 studies involving organic contaminant biodegradation, containing carbon and hydrogen
111 isotope measurements (Bennett et al. 2018, Cui et al. 2017, Elsner et al. 2007, Feisthauer
112 et al. 2011, Fischer et al. 2008, Holler et al. 2009, Hunkeler et al. 2001, Jaekel et al. 2014,
113 Kinnaman et al. 2007, Mancini et al. 2008, Mancini et al. 2003, McKelvie et al. 2009,
114 Rasigraf et al. 2012, Vogt et al. 2008, Zhang et al. 2019).
115

116 **Regression methods**

117 All calculations are performed in R using the native functions for OLR and the IsoPlotR
118 package for York regression and the pseudo code for the regressions was provided in the
119 previous literature (Ojeda et al. 2019).

120

121 **Method improvement**

122 The merits and demerits of existing calculation methods of Lambda were reviewed
123 carefully. Then winnow out the wheat from the mountains of chaff and attempt to develop
124 an improved method for Lambda calculation. Mainly by working hard to eradicate the
125 influence of the initial isotope signatures and non-reacting positions based on those
126 current methods.

127

128 **Evaluation effects**

129 By weighing up the relative merits of the modified method firstly and comparing of
130 Lambda values calculated with different methods, the validity of the new mathematical
131 model proposed. Specifically, five algorithms including four existing ones and one
132 derived here were used to calculate Lambda. All the calculated results were used for
133 evaluation the five methods, especially, the new approach (Table 1 and Fig. 1).

134

135 **Results and discussion**

136 **Merits/demerits of algorithms for Lambdas**

Lambda$_\alpha$ (Λ_α)

Mechanisms of various biochemical reactions could be compared straightforward, because distinct mechanisms usually lead to diverse Λ_αs. Besides, its major merit is elimination masking effect by commitment to catalysis. However, this method is rarely used in literature (Rasigraf et al. 2012). Firstly, the error of Λ_αs may increase after many operations from original data. An example can be found in the previous study (Feisthauer et al. 2011), where uncertainty is from 1.2 to 3.3, 11%–33% uncertainty in the calculated value of Λ_α (8.2–10.5). Furthermore, determining the precise fraction of remaining substrate (f) is necessary to calculate α_{rp} through Eq. (2). Actually, measurement of f is very difficult in the field investigation. Moreover, this method may be inappropriate for isotopes of high natural abundance (*e.g.*, S, Cl and so on), because it neglects the effect of molecules with more than one heavy isotope for isotope fractionation for the limited number of molecules (or low abundance molecules).

For a given reaction, the term on the right-hand-side of the Eq. (2) can be calculated based on the expected KIEs for different elements (Elsner et al. 2005). However, this has some limitations, which are largely due to the selection of the scope of KIE_C and KIE_H. Because of various transition states and masking effect of commitment to catalysis, apparent kinetic isotope effect of isotope fractionation tends to be variable in the same reaction mechanism.

Lambda$_{OLR}$ (Λ_{OLR})

The major advantage of Λ_{OLR} is that two-dimensional isotope plot could easily constructed even from field data, without measuring fraction of remaining substrate (*f*). Secondly, any two isotopes (even Br (Tang &Tan 2018), Cl (Rodriguez-Fernandez et al. 2018)) can been used to obtain Λ_{OLR} without the constraint of natural abundance. A third factor, it can be completed in one-step regression, thus reducing the transmission of errors. Last but not least, because Λ_{OLR} is approximately equal to Λ_{α} (Elsner et al. 2007, Vavilin &Rytov 2016) (derivation process in literature (Elsner et al. 2007) and revised below), distinct mechanisms usually lead to different Λ_{OLR} (Braeckevelt et al. 2012) Combined with the above advantages, Λ_{OLR} has been widely used involving two-dimensional isotopes (Badin et al. 2014, Solano et al. 2018) (or three (Kuder et al. 2013, Van Breukelen et al. 2017)).

However, there are still some flaws in this method. According to Eq. (1), first of all, the masking effect of commitment to catalysis on isotope fractionation is not linear. Therefore, it could not be eliminated exactly by simply through the ratio calculation. Especially in the case of high isotope fractionation (*e.g.*, ε >100‰), which is often observed with hydrogen isotope, the calculation of Λ_{OLR} is less reliable than Λ_{α} (Feisthauer et al. 2011). Furthermore, calculating Λ_{OLR} by OLR of $\Delta\delta E_1$ versus $\Delta\delta E_2$ has not been corrected with respect to nonreactive locations. This makes Λ_{OLR} deviate from Λ_{α} largely sometimes. Toluene degradation pathways by several anaerobic cultures

were investigated (Vogt et al. 2008) by 2D-CSIA. Λ_{OLR}, and Λ_{α} are showed in Table 1 and Fig. 1. Obviously, Λ_{OLR} is more than twice as much as Λ_{α}, which makes Λ_{OLR} can no longer to differentiate distinct mechanisms in this case. And Λ_{OLR}s cannot be compared with ones produced by other molecules in the same reaction type. However, there are only a few restrictions for Λ_{α} and one could be compared within distinct molecules reacted under similar reaction mechanism (Elsner et al. 2005). As a result, the relationship between $\Delta\delta E$ and Λ_{α} is reduced and Λ_{ri} and some other factors that may affect the accuracy of the dual-isotope plot is proposed.

Lambda$_{york}$ (Λ_{york})

Compared with Λ_{OLR}, Λ_{york} has some advantages, such as regression symmetry (Ojeda et al. 2019). Similar to Λ_{OLR}, nevertheless, the deviations between Λ_{york} and Λ_{α} are pronounced in some cases (Table 1 and Fig. 1), which point out that Λ_{york} needs to be further consummated.

Lambda$_{rp}$ (Λ_{rp})

Λ_{rp} take the influence of non-reacting positions into account and is much closer to Λ_{α} than Λ_{OLR} or Λ_{york} (Table1 and Fig. 1). However, this equation does not make much sense. On the one hand, Λ_{rp} does not completely eliminate masking effect by commitment to catalysis, unlike Λ_{α}. The relationship between Λ_{rp} and Λ_{α} is shown in Eq. (4) (derivation process provided in the Supplementary information).

$$\Lambda_{\alpha} = \frac{(\varepsilon_{rp,2}+1000)}{(\varepsilon_{rp,1}+1000)} \times \frac{\varepsilon_{rp,1}}{\varepsilon_{rp,2}} = \frac{(\varepsilon_{rp,2}+1000)}{(\varepsilon_{rp,1}+1000)} \times \Lambda_{rp} \quad (4)$$

On the other hand, Λ_{rp} has almost the same drawback with Λ_{α}, the precise fraction of remaining substrate must be determined and more calculation steps lead to greater uncertainties. Therefore, it's wiser to calculate Λ_{α} by Eq. (4) than $\varepsilon_{rp,1}/\varepsilon_{rp,2}$, if $\varepsilon_{rp,1}$ and $\varepsilon_{rp,2}$ are known.

Modified algorithm for Lambda

Eq. (5) (derivation processes were provided in the Supplementary information) is proposed to calculate Lambda (it is defined as Λ_{ri} in the present study), disadvantages mentioned above have been swept away. Here, York method is selected to regress $[(1000+\delta E_{0,2})*(n_1*x_2)*\Delta\delta E_{bulk,1}]$ versus $[(1000+\delta E_{0,1})*(n_2*x_1)*\Delta\delta E_{bulk,2}]$, since regression symmetry and the measurement error are accounted for in both variables, while error in the horizontal ordinate is ignored in OLR (Ojeda et al. 2019).

$$\Lambda_{ri} = \frac{n_1*x_2}{n_2*x_1} \times \frac{1000+\delta E_{0,2}}{1000+\delta E_{0,1}} \times \frac{\Delta\delta E_{bulk,1}}{\Delta\delta E_{bulk,2}} \quad (5)$$

Furthermore, Eq. (5) retains the advantages of two-dimension isotope plot, which has less uncertainty, no need to determine fraction of remaining substrate and can be constructed even from filed data. Most importantly, the deviation between Λ_{ri} calculated by Eq. (5)

221 and Λ_α is very small, even in the case of large deviation between Λ_α and Λ_{OLR} or Λ_{york}
222 (Table1 and Fig. 1). As a result, Λ_{ri} calculated by Eq. (5) is strongly recommended to
223 describe the relationship between two isotopes. And some factor that may affect the
224 accuracy of Λ_{ri} are discussed below.
225
226 **Merits of new method**
227 This method looks at many aspects of uncertainty of algorithm for Lambda at once.
228 Specifically, the improved method eliminates both the influences of non-reacting position
229 and the initial isotope signatures. At the same time, this method retains the advantages of
230 two-dimension isotope plot. For example, it eliminates contributions from commitment to
231 catalysis, but also no need to determine fraction of remaining substrate and can be
232 constructed even from filed data.
233
234 The isotope signature measured with GC-IRMS can only provide average bulk isotope
235 ratios, in which the changes will be smaller than those at the reacting positions. In several
236 molecules, there is little different between Λ_{ir} and Λ_{OLR} or Λ_{york}. In the enrichment of ^{13}C
237 and ^{2}H during monooxygenase-mediated biodegradation of 1,4-dioxane(Bennett et al.
238 2018), 1,4-dioxane is the target molecule and C and H considered elements, n_C=8, n_H=8,
239 x_C=4, x_H=4, so $\frac{n_1 * x_2}{n_2 * x_1} = 1$. Nevertheless, in most cases, $\frac{n_1 * x_2}{n_2 * x_1}$ is not equal to one, and
240 some even deviate greatly. For toluene in Table 1 and Fig. 1, the deviation is 38.1%.
241

242 One may say that the determination of n and x will complicate the analysis. However, this
243 step is necessary. Λs obtained by average bulk isotope ratios (Λ_{OLR} or Λ_{york}) implies a
244 hypothesis that all atoms of considered element in the molecule are in reactive positions.
245 On the other hand, distinct molecule usually present diverse values of $\frac{n_1 * x_2}{n_2 * x_1}$, which
246 greatly restrict the comparison between them, even if similar reaction mechanism is
247 occurring. The transformation of Λ_{OLR} or Λ_{york} into Λ_{ri} make it convenient to compare
248 with each other, irrespective of their molecular size. For the same biochemical reaction,
249 Λ_{ri} could be compared in different, even for structurally very dissimilar contaminants.
250
251 In one-dimensional CSIA data processing, practitioners often ignore the effect of the
252 initial isotope signatures, but focus more on the range of measured delta values. However,
253 different initial isotope values may lead to different conclusions. The theoretical
254 derivation about it and an example are given in the Supplementary information. Similarly,
255 the initial isotope signatures have a certain influence on the two-dimensional CSIA data
256 processing. In general, the initial isotope signatures ratio ($\frac{1000+\delta E_{0,2}}{1000+\delta E_{0,1}}$) are very close to
257 unity and have a minimal impact on Λs. The mathematical error is less than 5% when the
258 deviation between $\delta E_{0,1}$ and $\delta E_{0,2}$ is less than 50‰ ($|\delta E_{0,1} - \delta E_{0,2}| < 50‰$). The
259 effect is ignored when dealing data in the overwhelming majority of papers and the
260 information about initial isotope signature provided in some literature is shown in Table
261 S1. However, negative situation may emerge in some cases. The changes of carbon and
262 hydrogen isotope signatures of ethane during aerobic biodegradation was investigated

(Kinnaman et al. 2007), δ^2H_0 and $\delta^{13}C_0$ is about -32.1‰ and -347‰. And the arithmetic result of $(1000 + \delta E_{0,C})/(1000 + \delta E_{0,H})$ is 148%. In other words, the impact of initial isotope signatures may cause Λs to deviate by 48%. In addition, due to different original sources and production procedures, the initial isotope signature used in each laboratory and between organics are various, which limits the comparison of Λs between different laboratories and molecules. Plus, $(1000 + \delta E_{0,2})/(1000 + \delta E_{0,1})$ is easy to get, the initial isotope signatures are strongly recommended to take into account.

Implications for reaction mechanisms

Λ_{ri} estimated with our approach and Λ_{OLR} are very different in some case. However, the deviation between them is smaller after multiplying Λ_{OLR} by $\frac{n_1*x_2}{n_2*x_1}$ (Table 2). Therefore, in the future research, Λ_{OLR} corrected by $\frac{n_1*x_2}{n_2*x_1}$ also have certain comparability in similar reaction mechanisms.

The relationship between Λ and KIE (Eq. (6)) is derived in previous literature (Elsner et al. 2005). KIE is mechanism-specific (Ojeda et al. 2019), so Λ_{ri} could be comparable for the identical mechanism with same Z.

$$\Lambda_\alpha = \frac{KIE_H - 1}{KIE_C - 1} \times \frac{1 + KIE_C(Z_C - 1)}{1 + KIE_H(Z_H - 1)} \quad (6)$$

where Z is the number of indistinguishable atoms in intramolecular competition.

When a set of Λ_{ri}s from certain known reaction are collected, the 95 percent confidence interval will generate through one sample *t* test. If the value of individual Λ_{ri} measured from any unknown reaction fall within the confidence interval, they are likely to act with the same reaction mechanism. Therefore, it is necessary to collect sets of Λ_{ri}s from certain known reactions (Table S2 in Supplementary information) and to generate the 95 percent confidence interval. The range of 5.67–24.8, 8.54–9.80, 0.51–8.35, 25.2–36.8, 7.09–21.9 are responsible for oxidation of C-H bonds (Z_C=1, Z_H=3), oxidation of C-H bonds (Z_C=1,Z_H=4), aerobic biodegradation of benzene (Z_C=6,Z_H=6), methanogenic or sulfate-reducing biodegradation of benzene (Z_C=6,Z_H=6), and nitrate-reducing biodegradation of benzene (Z_C=6,Z_H=6). In the case of C-H bond oxidation, some values of Λ_{ri} is not in the range of 5.67–24.8 (such as Λ_{ri}=40.3 (McKelvie et al. 2009), 4.19 (Vogt et al. 2008)). For the larger values, it may be due to the hydrogen secondary isotope effect, which cause strong hydrogen isotope fractionation (Elsner et al. 2007), therefore bigger Λ_{ri}s.

Form another point of view, one sample *t* test focuses on the overall data, not on particularly high or low values of Λ_{ri}s that may theoretically be outliers of the data group. Nevertheless, due to the limited sample data, the range set for various reaction mechanism may be a little inaccurate. In the future research, more date from various reaction mechanism could be collected to generate the 95 percent confidence interval of all mechanisms.

Conclusions

A method to calculate dual-isotope slope (Λ) with less uncertainty is crucial to monitor transformation processes. Owing to the deficiencies of the current methods of calculating Λ, inaccurate conclusions may be drawn. Λ is calculated by our method (Λ_{ri}), which take the influence of non-reacting position and the initial isotope signatures into account, leading to an appropriate estimation of Λ and its uncertainty. The ranges of Λ_{ri} values responsible for a specific reaction mechanism are generated using the student's *t* test. These ranges facilitate the judgment of reaction mechanism in field. This set of best practices will help practitioners select the appropriate method to process the data of 2D CSIA and apply it to the natural attenuation of organic pollutants in the environment.

Declarations

Ethics approval and consent to participate

Not applicable.

Consent for publication

Not applicable.

Availability of data and materials

All data generated or analysed during this study are included in this published article and

its supplementary information files.

Competing interests

The authors declare that they have no competing interests.

Funding

This study was financially supported by the National Natural Science Foundation of China (No. 21876004).

Authors' contributions

Jin-Ru Feng: Investigation, Data curation, Writing - original draft. Hong-Gang Ni: Validation, Supervision, Writing - review & editing, funding acquisition. All authors read and approved the final manuscript.

Supplementary information

The online version contains Supplementary material available at https://doi.org/xxxx.

References

Badin A, Buttet G, Maillard J, Holliger C, Hunkeler D (2014) Multiple dual C-Cl isotope patterns associated with reductive dechlorination of tetrachloroethene. Environ Sci Technol 48:9179–9186. https://doi.org/10.1021/es500822d.

Bennett P, Hyman M, Smith C, El Mugammar H, Chu M-Y, Nickelsen M, Aravena R (2018) Enrichment with carbon-13 and deuterium during monooxygenase-mediated biodegradation of 1,4-dioxane. Environmental Science and Technology Letters 5:148–153. https://doi.org/10.1021/acs.estlett.7b00565.

Braeckevelt M, Fischer A, Kastner M (2012) Field applicability of compound-specific isotope analysis (CSIA) for characterization and quantification of in situ contaminant degradation in aquifers. Applied Microbiology and Biotechnology 94:1401–1421. https://doi.org/10.1007/s00253-012-4077-1.

Cui MC, Zhang WB, Fang J, Liang QQ, Liu DX (2017) Carbon and hydrogen isotope fractionation during aerobic biodegradation of quinoline and 3-methylquinoline. Applied Microbiology and Biotechnology 101:6563–6572. https://doi.org/10.1007/s00253-017-8379-1.

Elsner M, Zwank L, Hunkeler D, Schwarzenbach RP (2005) A new concept linking observable stable isotope fractionation to transformation pathways of organic pollutants. Environ Sci Technol 39:6896–6916. https://doi.org/10.1021/es0504587.

Elsner M, Mckelvie J, Couloume GL, Lollar BS (2007) Insight into methyl tert-butyl ether (MTBE) stable isotope Fractionation from abiotic reference experiments. Environ Sci Technol 41:5693–5700. https://doi.org/10.1021/es070531o.

Elsner M (2010) Stable isotope fractionation to investigate natural transformation mechanisms of organic contaminants: principles, prospects and limitations. Journal of Environmental Monitoring 12:2005–2031. https://doi.org/10.1039/c0em00277a.

Elsner M, Imfeld G (2016) Compound-specific isotope analysis (CSIA) of micropollutants in the environment - current developments and future challenges. Current Opinion in Biotechnology 41:60–72. https://doi.org/10.1016/j.copbio.2016.04.014.

Feisthauer S, Vogt C, Modrzynski J, Szlenkier M, Kruger M, Siegert M, Richnow HH (2011) Different types of methane monooxygenases produce similar carbon and hydrogen isotope fractionation patterns during methane oxidation. Geochim Cosmochim Ac 75:1173–1184. https://doi.org/10.1016/j.gca.2010.12.006.

Fischer A, Theuerkorn K, Stelzer N, Gehre M, Thullner M, Richnow HH (2007) Applicability of

376 stable isotope fractionation analysis for the characterization of benzene biodegradation in a
377 BTEX-contaminated aquifer. Environ Sci Technol 41:3689–3696.
378 https://doi.org/10.1021/es061514m.

379 Fischer A, Herklotz I, Herrmann S, Thullner M, Weelink SAB, Stams AJM, Schlomann M,
380 Richnow HH, Vogt C (2008) Combined carbon and hydrogen isotope fractionation
381 investigations for elucidating benzene biodegradation pathways. Environ Sci Technol
382 42:4356–4363. https://doi.org/10.1021/es702468f.

383 Holler T, Wegener G, Knittel K, Boetius A, Brunner B, Kuypers MMM, Widdel F (2009)
384 Substantial C-13/C-12 and D/H fractionation during anaerobic oxidation of methane by
385 marine consortia enriched in vitro. Environmental Microbiology Reports 1:370–376.
386 https://doi.org/10.1111/j.1758-2229.2009.00074.x.

387 Hunkeler D, Anderson N, Aravena R, Bernasconi SM, Butler BJ (2001) Hydrogen and carbon
388 isotope fractionation during aerobic biodegradation of benzene. Environ Sci Technol
389 35:3462–3467. https://doi.org/10.1021/es0105111.

390 Jaekel U, Vogt C, Fischer A, Richnow HH, Musat F (2014) Carbon and hydrogen stable isotope
391 fractionation associated with the anaerobic degradation of propane and butane by marine
392 sulfate-reducing bacteria. Environmental Microbiology 16:130–140.
393 https://doi.org/10.1111/1462-2920.12251.

394 Kinnaman FS, Valentine DL, Tyler SC (2007) Carbon and hydrogen isotope fractionation
395 associated with the aerobic microbial oxidation of methane, ethane, propane and butane.
396 Geochim Cosmochim Ac 71:271–283. https://doi.org/10.1016/j.gca.2006.09.007.

397 Kuder T, van Breukelen BM, Vanderford M, Philp P (2013) 3D-CSIA: Carbon, Chlorine, and
398 Hydrogen Isotope Fractionation in Transformation of ICE to Ethene by a Dehalococcoides
399 Culture. Environ Sci Technol 47:9668–9677. https://doi.org/10.1021/es400463p.

400 Mancini SA, Ulrich AC, Lacrampe-Couloume G, Sleep B, Edwards EA, Lollar BS (2003) Carbon
401 and hydrogen isotopic fractionation during anaerobic biodegradation of benzene. Applied and
402 Environmental Microbiology 69:191–198. https://doi.org/10.1128/AEM.69.1.191-198.2003.

403 Mancini SA, Devine CE, Elsner M, Nandi ME, Ulrich AC, Edwards EA, Lollar BS (2008)
404 Isotopic evidence suggests different initial reaction mechanisms for anaerobic benzene
405 biodegradation. Environ Sci Technol 42:8290–8296. https://doi.org/10.1021/es801107g.

406 McKelvie JR, Hyman MR, Elsner M, Smith C, Aslett DM, Lacrampe-Couloume G, Lollar BS
407 (2009) Isotopic fractionation of methyl *tert*-butyl ether suggests different initial reaction
408 mechanisms during aerobic biodegradation. Environ Sci Technol 43:2793–2799.
409 https://doi.org/10.1021/es803307y.

Northrop DB (1981) The Expression of Isotope Effects on Enzyme-Catalyzed Reactions. Annual Review of Biochemistry 50:103–131. https://doi.org/10.1146/annurev.bi.50.070181.000535.

Ojeda AS, Phillips E, Mancini SA, Lollar BS (2019) Sources of Uncertainty in Biotransformation Mechanistic Interpretations and Remediation Studies using CSIA. Analytical Chemistry 91:9147–9153. https://doi.org/10.1021/acs.analchem.9b01756.

Rasigraf O, Vogt C, Richnow HH, Jetten MSM, Ettwig KF (2012) Carbon and hydrogen isotope fractionation during nitrite-dependent anaerobic methane oxidation by methylomirabilis oxyfera. Geochim Cosmochim Ac 89:256–264. https://doi.org/10.1016/j.gca.2012.04.054.

Rodriguez-Fernandez D, Torrento C, Palau J, Marchesi M, Soler A, Hunkeler D, Domenech C, Rosell M (2018) Unravelling long-term source removal effects and chlorinated methanes natural attenuation processes by C and Cl stable isotopic patterns at a complex field site. Science of the Total Environment 645:286–296. https://doi.org/10.1016/j.scitotenv.2018.07.130.

Solano FM, Marchesi M, Thomson NR, Bouchard D, Aravena R (2018) Carbon and Hydrogen Isotope Fractionation of Benzene, Toluene, and o-Xylene during Chemical Oxidation by Persulfate. Ground Water Monitoring and Remediation 38:62–72. https://doi.org/10.1111/gwmr.12228.

Tang CM, Tan JH (2018) Simultaneous observation of concurrent two-dimensional carbon and chlorine/bromine isotope fractionations of halogenated organic compounds on gas. Analytica Chimica Acta 1039:172–182. https://doi.org/10.1016/j.aca.2018.07.015.

Van Breukelen BM, Thouement HAA, Stack PE, Vanderford M, Philp P, Kuder T (2017) Modeling 3D-CSIA data: Carbon, chlorine, and hydrogen isotope fractionation during reductive dechlorination of TCE to ethene. J Contam Hydrol 204:79–89. https://doi.org/10.1016/j.jconhyd.2017.07.003.

Vavilin VA, Rytov SV (2016) Inhibition by Nitrite Ion in the Process of Methane Anaerobic Oxidation by Microorganisms and Fractionation Dynamics of Stable Carbon and Hydrogen Isotopes. Water Resources 43:663–667. https://doi.org/10.1134/S0097807816040163.

Vogt C, Cyrus E, Herklotz I, Schlosser D, Bahr A, Herrmann S, Richnow HH, Fischer A (2008) Evaluation of toluene degradation pathways by two-dimensional stable isotope fractionation. Environ Sci Technol 42:7793–7800. https://doi.org/10.1021/es8003415.

Zhang D, Wu LP, Yao J, Vogt C, Richnow HH (2019) Carbon and hydrogen isotopic fractionation during abiotic hydrolysis and aerobic biodegradation of phthalate esters. Science of the Total Environment 660:559–566. https://doi.org/10.1016/j.scitotenv.2019.01.003.

Zwank L, Berg M, Elsner M, Schmidt TC, Schwarzenbach RP, Haderlein SB (2005) New evaluation scheme for two-dimensional isotope analysis to decipher biodegradation processes: Application to groundwater contamination by MTBE. Environ Sci Technol 39:1018–1029. https://doi.org/10.1021/es049650j.

448 **Table 1** Compare of Λ values calculated using different methods.

	Λ_{α}	Λ_{OLR}	Λ_{york}	Λ_{rp}	Λ_{ri}	References
Anaerobic biodegradation of toluene[1]	4.98	11.0		4.63	4.19[a]	(Vogt et al. 2008)
	5.99	15.0		5.05	5.71[a]	
	6.06	14.0		5.50	5.33[a]	
	2.14	4.00		2.07	1.52[a]	
	12.7	28.0		10.5	10.7[a]	
	12.6	31.0		10.9	11.8[a]	
	14.6	27.0		11.7	10.3[a]	
Aerobic biodegradation of DMP[2]	1.57	5.30	5.73[b]	1.55	1.94[b]	(Zhang et al. 2019)
Aerobic biodegradation of DEP[2]	1.95	2.60	2.70[b]	1.90	1.58[b]	(Zhang et al. 2019)
Anaerobic biodegradation of propane[3]	8.16	6.30		7.72	8.40[a]	(Jaekel et al. 2014)
	14.0	11.9		10.6	15.9[a]	
	10.4	7.90		9.57	10.5[a]	
	13.4	10.0		11.8	13.3[a]	
Anaerobic biodegradation of butane[4]	6.11	4.90		6.00	6.13[a]	(Jaekel et al. 2014)
	7.99	6.90		7.47	8.63[a]	
	7.17	5.90		7.00	7.38[a]	
	11.0	8.70		9.91	10.9[a]	
	8.09	5.30		8.00	6.63[a]	
	9.93	7.70		9.67	9.63[a]	
Aerobic biodegradation of 1,4-dioxane[5]	7.92	7.50	9.31		9.31	(Bennett et al. 2018)
	11.5	10.9	11.2		11.2	
	36.5	37.2	39.1		39.1	

449 [1] Seven different microbial strains reacted by benzylsuccinate synthase. [2] *Rhodococcus opacus DSM 43250* reacted by S_N2 reactions.
450 [3] Two different microbial strains reacted by oxidation of C-H bond. [4] Three different microbical strains reacted by oxidation of C-H
451 bond. [5] Two different microbial strains reacted by oxidation of C-H bond.

[a] Approximated by $\Lambda_{ri} \approx \frac{n_1 * x_2}{n_2 * x_1} \times \Lambda_{\mathrm{OLR}} \times \frac{1000+\delta E_{0,2}}{1000+\delta E_{0,1}}$ and $\frac{1000+\delta E_{0,2}}{1000+\delta E_{0,1}} \approx 1$ here. [b] Raw data is obtained by visual inspection from the figures in the literature. DMP: Dimethyl phthalate; DEP: Diethyl phthalate; MTBE: methyl *tert*-butyl ether.

455 **Table 2** Comparison of Λ_{OLR}s and Λ_{ri}s calculated with the proposed method in the present study.

	Λ_{OLR}	$(n_1x_2/n_2x_1)\times\Lambda_{OLR}$	Λ_{ri}	References
Aerobic biodegradation of DMP	5.30±0.4	1.77±0.1	1.94±0.1[a]	(Zhang et al. 2019)
Aerobic biodegradation of DEP	2.60±0.5	1.52±0.3	1.58±0.9[a]	(Zhang et al. 2019)
MTBE Acid Hydrolysis	11.1±1.3	2.96±0.3	2.99±0.3	(Elsner et al. 2007)
Aerobic biodegradation of 1,4-dioxane	10.9±2.2[b]	10.9±2.2	11.2±1.2	(Bennett et al. 2018)
	37.2±2.6[c]	37.2±2.6	39.1±1.8	

456 [a] Raw data is obtained by visual inspection from the figures in the literature; DMP: Dimethyl phthalate; DEP: Diethyl phthalate;
457 MTBE: methyl tert-butyl ether; [b] strain: *R. rhodochrous ATCC 21198*, growth substrate: isobutene; [c] strain:*P. tetrahydrofuranoxidans*
458 K1, growth substrate: tetrahydrofuran.

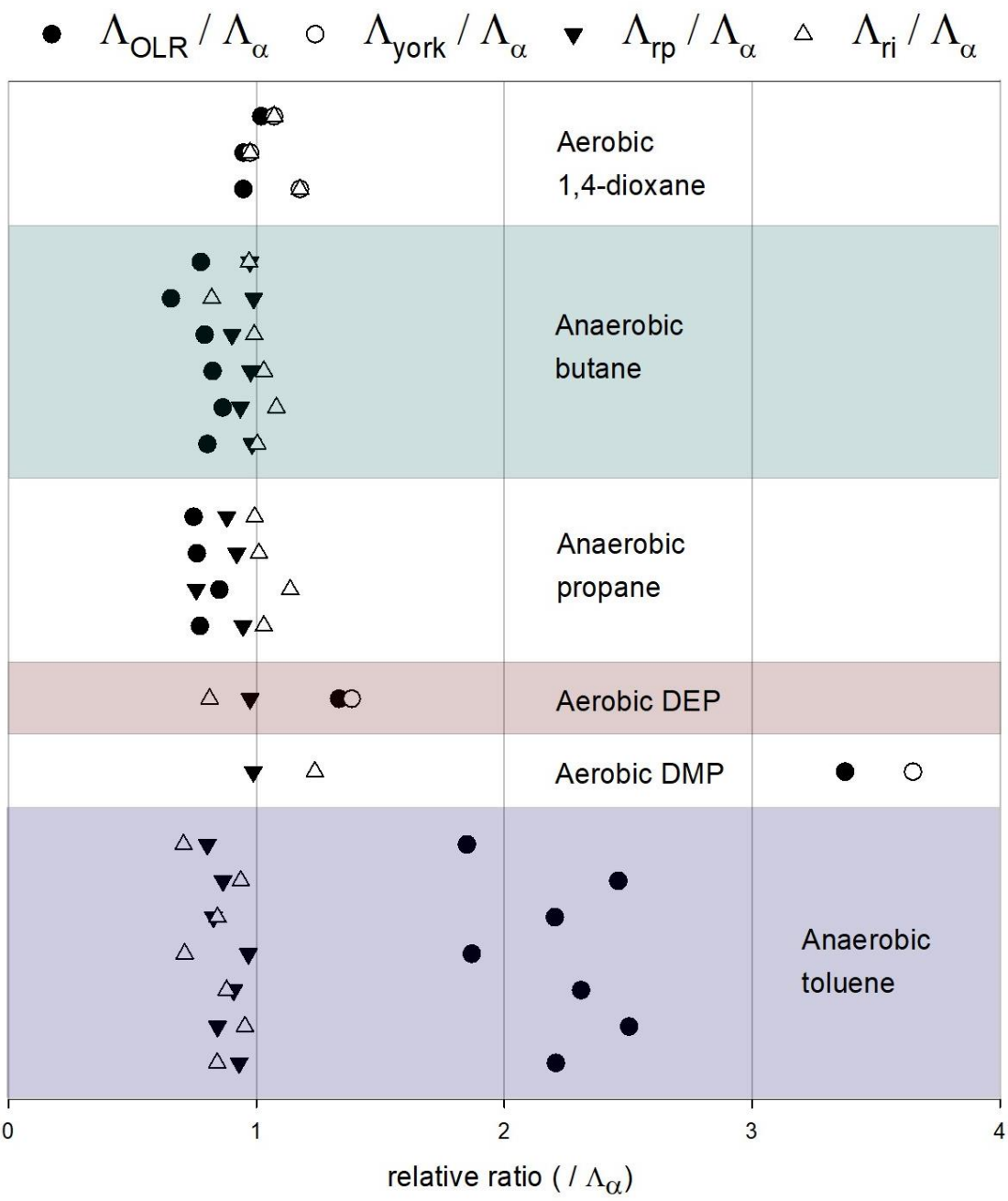

Fig. 1 Compare of Λ calculated using different methods. Relative ratio (/ Λ_{α}) are calculated with dividing different types of Λ values by the corresponding value of Λ_{α} (listed in Table 1). "anaerobic biodegradation of toluene", "aerobic biodegradation of DMP", "aerobic biodegradation of DEP", "anaerobic degradation of propane" and "aerobic degradation of 1,4-dioxane" are abbreviated as "anaerobic toluene", "aerobic DMP", "aerobic DEP", "anaerobic propane" and "aerobic 1,4-dioxane", respectively.

Figures

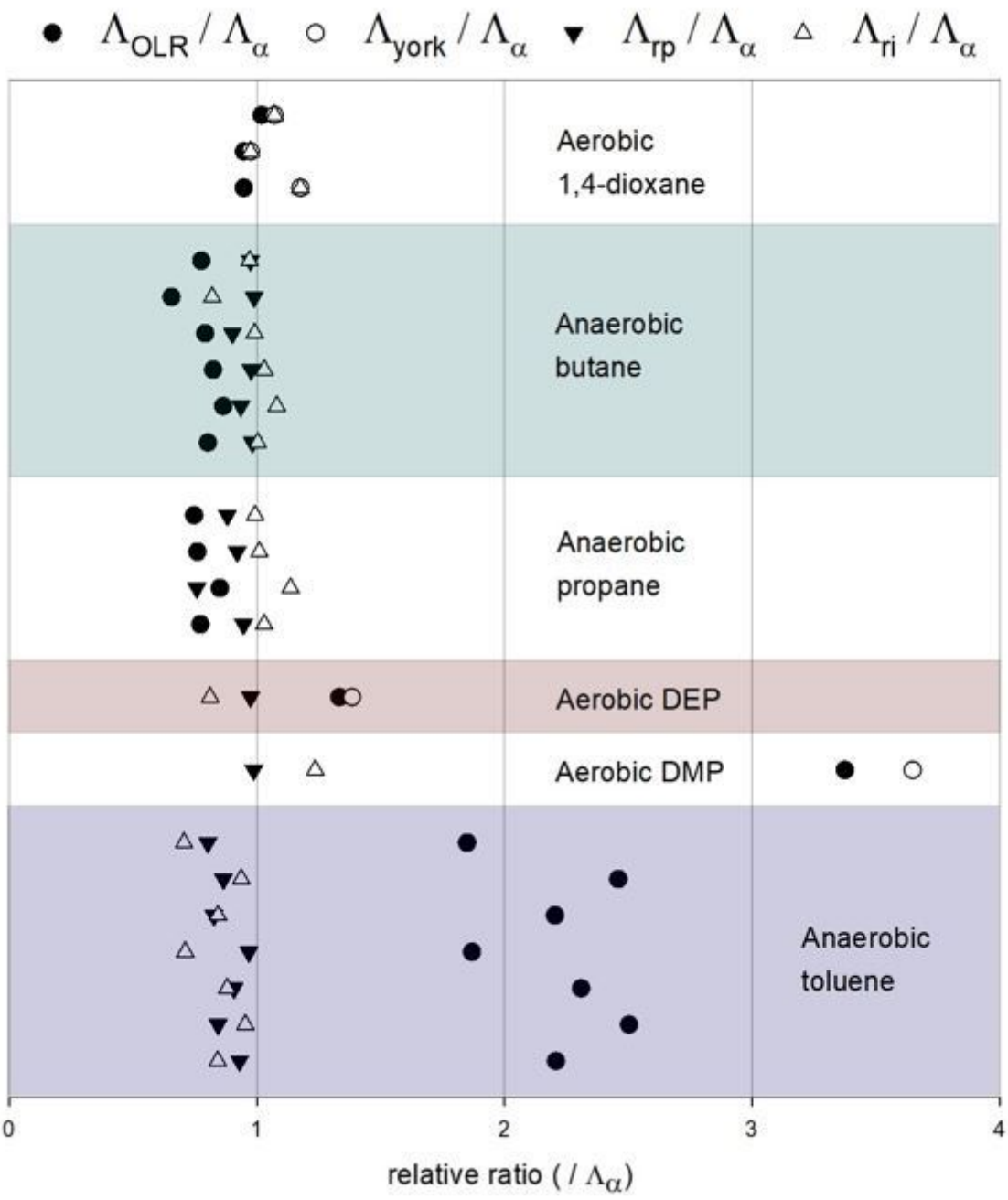

Figure 1

Compare of Λ calculated using different methods. Relative ratio (/ Λα) are calculated with dividing different types of Λ values by the corresponding value of Λα (listed in Table 1). “anaerobic biodegradation of toluene”, “aerobic biodegradation of DMP”, “aerobic biodegradation of DEP”, “anaerobic degradation of propane” and “aerobic degradation of 1,4-dioxane” are abbreviated as “anaerobic toluene”, “aerobic DMP”, “aerobic DEP”, “anaerobic propane” and “aerobic 1,4-dioxane”, respectively.